

UCLA

UCLA Previously Published Works

Title

Optimizing Collagen Scaffolds for Bone Engineering

Permalink

<https://escholarship.org/uc/item/2fb5h3vx>

Journal

Journal of Craniofacial Surgery, 26(6)

ISSN

1049-2275

Authors

Lee, Justine C
Pereira, Clifford T
Ren, Xiaoyan
et al.

Publication Date

2015-09-01

DOI

10.1097/scs.0000000000001918

Peer reviewed



Published in final edited form as:

J Craniofac Surg. 2015 September ; 26(6): 1992–1996. doi:10.1097/SCS.0000000000001918.

Optimizing Collagen Scaffolds for Bone Engineering: Effects of Cross-linking and Mineral Content on Structural Contraction and Osteogenesis

Justine C. Lee, MD, PhD^{*†}, Clifford T. Pereira, MBBS^{*†}, Xiaoyan Ren, MD, PhD^{*†}, Weibiao Huang, PhD^{*†}, David Bischoff, PhD[‡], Daniel W. Weisgerber, BA[§], Dean T. Yamaguchi, MD, PhD[‡], Brendan A. Harley, ScD[§], and Timothy A. Miller, MD^{*†}

^{*}Division of Plastic and Reconstructive Surgery, UCLA David Geffen School of Medicine, Los Angeles, CA

[†]Division of Plastic and Reconstructive Surgery, Greater Los Angeles VA Healthcare System, Los Angeles, CA

[‡]Research Service, Greater Los Angeles VA Healthcare System, Los Angeles, CA

[§]Department of Chemical and Biomolecular Engineering, Institute for Genomic Biology, University of Illinois at Urbana-Champaign, Urbana, IL

Abstract

Introduction—Osseous defects of the craniofacial skeleton occur frequently in congenital, posttraumatic, and postoncologic deformities. The field of scaffold-based bone engineering emerged to address the limitations of using autologous bone for reconstruction of such circumstances. In this work, the authors evaluate 2 modifications of three-dimensional collagen-glycosaminoglycan scaffolds in an effort to optimize structural integrity and osteogenic induction.

Methods—Human mesenchymal stem cells (hMSCs) were cultured in osteogenic media on nonmineralized collagen-glycosaminoglycan (C-GAG) and nanoparticulate mineralized collagen-glycosaminoglycan (MC-GAG) type I scaffolds, in the absence and presence of cross-linking. At 1, 7, and 14 days, mRNA expression was analyzed using quantitative real-time-reverse-transcriptase polymerase chain reaction for osteocalcin (OCN) and bone sialoprotein (BSP). Structural contraction was measured by the ability of the scaffolds to maintain their original dimensions. Mineralization was detected by microcomputed tomographic (micro-CT) imaging at 8 weeks. Statistical analyses were performed with Student *t*-test.

Results—Nanoparticulate mineralization of collagen-glycosaminoglycan scaffolds increased expression of both OCN and BSP. Cross-linking of both C-GAG and MC-GAG resulted in decreased osteogenic gene expression; however, structural contraction was significantly decreased after cross-linking. Human mesenchymal stem cells-directed mineralization, detected by micro-

Address correspondence and reprint requests to Justine C. Lee, MD, PhD, UCLA Division of Plastic and Reconstructive Surgery, 200 UCLA, Medical Plaza, Suite 465, Los Angeles, CA 90095; ; Email: justine@ucla.edu.

The authors report no conflicts of interest.

CT, was increased in nanoparticulate mineralized scaffolds, although the density of mineralization was decreased in the presence of cross-linking.

Conclusions—Optimization of scaffold material is an essential component of moving toward clinically translatable engineered bone. Our current study demonstrates that the combination of nanoparticulate mineralization and chemical cross-linking of C-GAG scaffolds generates a highly osteogenic and structurally stable scaffold.

Keywords

Bone engineering; mesenchymal stem cells; nanoparticulate mineralized collagen scaffolds

Congenital, posttraumatic, and postoncologic skeletal defects are currently treated using autologous bone grafts, which are fraught with considerable limitations, such as significant donor site morbidity, limited tissue availability, bleeding, infection, and chronic pain.^{1,2} Laboratory-engineered bone has been an important and exciting endeavor as an alternative to autologous or allogenic bone grafts. To date, numerous two- and three-dimensional in vitro models of bone graft substitutes have been described.^{3,4} Our current challenge lies in efficiently screening and optimizing the osteogenic potential of such bone biomaterials for bioactivity using clinically relevant models.

Effective strategies for bone engineering generally require 2 components: cellular material and extracellular matrix. These components frequently manifest as mesenchymal stem cells and bioengineered scaffolds, respectively. We have previously shown that scaffold material affects in vitro mineralization.⁵ Our study demonstrated that human mesenchymal stem cells (hMSCs) seeded on nonmineralized collagen-glycosaminoglycan (C-GAG) scaffolds exhibit accelerated and robust mineralization in comparison to synthetic poly L-lactide-co-glycolide (PLGA). We also discovered that cell-seeded collagen scaffolds, however, undergo significant contraction compared with PLGA scaffolds.⁵ Given the need to maintain porosity to allow for efficient cell penetration into the scaffold as well as sufficient diffusion-based biotransport of nutrients and oxygen to maintain cell activity, this contraction may significantly impair the use of collagen implants in repairing bony defects in vivo. Furthermore, given recent observations linking loss of differentiated cell phenotype with cell mediated-contraction of C-GAG scaffolds,⁶ it is important to examine and gain an improved understanding of how scaffold contraction impacts osteogenesis.

Despite promising results with collagen scaffolds, our previous work clearly demonstrated that clinical translation required additional modifications and optimization of collagen scaffolds. Cross-linking collagen and GAG has been shown to increase the structural integrity and stiffness of the resultant scaffold (XC-GAG) in biomechanical studies.^{7,8} In addition, we (Brendan A. Harley) have also recently designed and fabricated a mineralized collagen-glycosaminoglycan (MC-GAG) scaffold using a coprecipitation approach that induces precipitation of calcium phosphate (CaP) crystallites together with collagen and GAGs to form nanoparticulate mineralized content on the collagen fibrils.⁷ This latter modification results in a production of a scaffold that mimics native bone composition and which can support long term expansion of human mesenchymal stem cells.⁹

In this work, we investigate the effects of cross-linking and nanoparticulate mineralization of C-GAG scaffolds on osteogenic gene expression and mineralization of human mesenchymal stem cells in preparation for clinical translation.

METHODS

Fabrication of Nonmineralized Collagen Scaffolds

Collagen-glycosaminoglycan scaffolds were prepared using the lyophilization process described previously.⁸ Briefly, a suspension of collagen and GAGs were produced by combining microfibrillar, type I collagen (0.5 wt %) isolated from bovine tendon (Collagen Matrix, Oakland, NJ) and chondroitin-6-sulfate (0.05 wt %) isolated from shark cartilage (Sigma-Aldrich, St. Louis, MO) in a solution of 0.05 M acetic acid (pH 3.2). The suspension was frozen using a constant cooling rate technique (1°C/min) from room temperature to a final freezing temperature of -10°C using a freeze dryer (Genesis, VirTis). The ice phase was sublimated under vacuum (<200 mTorr, 0°C). Disks 8 mm in diameter and 3.5 mm in thickness (density 0.0071 ± 0.0008 g/cm³) were prepared using punch biopsies for cultures.

Fabrication of Mineralized Collagen Scaffolds

Mineralized C-GAG scaffolds were prepared using the lyophilization process previously described.^{7,8} Briefly, a suspension of collagen-glycosaminoglycan-calcium phosphate (CGCaP) was produced by combining microfibrillar, type I collagen (1.9 wt %) isolated from bovine tendon (Collagen Matrix), chondroitin-6-sulfate (0.17 wt %) isolated from shark cartilage (Sigma-Aldrich), and calcium salts (calcium nitrate hydrate: Ca(NO₃)₂·4H₂O; calcium hydroxide: Ca(OH)₂, Sigma-Aldrich) in a solution of phosphoric acid. The CGCaP suspension lyophilized using identical process conditions as the nonmineralized C-GAG scaffolds. Disks 8 mm in diameter and 3.5 mm in thickness (density 0.0548 ± 0.0045 g/cm³) were prepared using punch biopsies for cultures.

Chemical Cross-Linking of Mineralized and Nonmineralized Collagen Scaffolds

Non-mineralized scaffolds (C-GAG) and mineralized scaffolds (MC-GAG) were weighed before chemical cross-linking. These were placed into 100% ethanol under a laminar flow hood and left overnight. The scaffolds were then placed in serial dilutions of ethanol and phosphate buffered saline (PBS, Sigma-Aldrich) every 2 hours, to a final solution of 100% PBS, then allowed to hydrate overnight. Scaffolds were then immersed in a solution of 1-ethyl-3-(3-dimethylaminopropyl) carbodiimide (EDAC, Sigma-Aldrich) and *N*-hydroxysuccinimide (NHS, Sigma-Aldrich) in distilled, deionized water for 2 hours at room temperature.¹⁰ After cross-linking, the scaffolds were washed in fresh PBS for an additional 2 hours to remove any remaining chemical.

Cell Culture

Human mesenchymal stem cells were purchased and cultured according to the manufacturer's specifications (Lonza, Inc., Allendale, NJ) in hMSC growth media in humidified 5% CO₂/95% air at 37°C and were used below passage 10. Cells (2.5×10^5 cells per scaffold) were seeded onto collagen scaffolds, allowed to attach for 1 hour, and incubated overnight in hMSC growth media to allow acclimatization using a previously

described static seeding method.¹¹ After 24 hours, the scaffolds were subjected to osteogenic differentiation medium, composed of hMSC growth media plus 10 mM β -glycerol phosphate, 50 μ g/mL ascorbic acid, and 0.1 μ M dexamethasone. All chemicals were purchased from Sigma-Aldrich (St. Louis, MO). Culture medium was changed every 2 to 3 days. At 5 weeks of culture, diameters of scaffolds were measured and recorded in triplicate.

Quantitative Real-Time Reverse-Transcriptase Polymerase Chain Reaction

Scaffolds were processed for total RNA extraction using the RNeasy kit (Qiagen, Valencia, CA) at 1, 7, and 14 days. Gene sequences for 18S rRNA, osteocalcin (OCN), and bone sialoprotein (BSP) were obtained from the National Center for Biotechnology Information gene database and oligonucleotide primers designed (Table 1). Quantitative real-time reverse-transcriptase polymerase chain reaction (RT-PCR) was performed on the Opticon Continuous Fluorescence System (Bio-Rad Laboratories, Inc., Hercules, CA) using the QuantiTect SYBR Green RT-PCR kit (Qiagen). Cycle conditions were as follows: reverse transcription at 50°C (30 minutes); activation of HotStarTaq DNA polymerase/inactivation of reverse transcriptase at 95°C (15 minutes); and 45 cycles of 94°C for 15 seconds, 58°C for 30 seconds, and 72°C for 45 seconds. 18S rRNA was used to normalize the amount of template for each sample. Each reaction was run in triplicate. Results were analyzed using the comparative CT method for analyzing reverse-transcriptase polymerase chain reaction data and presented as representative graphs of triplicate experiments.

Microcomputed Tomographic Imaging

Mineralization was followed by microcomputed tomographic imaging (micro-CT) using the Scanco micro-CT 35 (Scanco Medical AG, Bruttisellen, Switzerland) at 8 weeks in culture (N = 3 scaffolds per time point) in the same conditions described above. Scaffolds were fixed using 10% formalin for 24 hours and stored in 70% ethanol at 4°C. Scans were performed using medium resolution settings with a source voltage of 70 E (kVp) and I (μ A) of 114. The images had a final element size of 12.5 μ m. Two-dimensional images were analyzed using software supplied from Scanco (Image Processing Language version 5.6). Scaffold areas were contoured to establish volumes of interest by visual examination of serial slices in all of the specimens. Optimum arbitrary threshold values of 20 (showing scaffold and mineralization) and 80 (mineralization alone) were used uniformly for all specimens to quantify mineralized areas from surrounding unmineralized scaffold.

Histomorphometric analysis of three-dimensional reconstructions was performed using Scanco Evaluation scripts no. 2 (three-dimensional segmentation of 2 volumes of interest: solid dense in transparent low-density object) for three-dimensional images and script no. 6 (bone volume/density only bone evaluation) for volume determinations.

Statistical Analysis

Computer-assisted statistical analyses were performed using SigmaStat 3.5 (Systat Software, Inc., San Jose, CA). Data points were composed of duplicates of at least 3 independent experiments, unless otherwise indicated. Mean measurements of mRNA expression were analyzed for statistical significance by either analysis of variance or independent Student *t*-test, as appropriate. A value of $P < 0.05$ was considered significant.

RESULTS

Nanoparticulate Mineralization of Collagen-Glycosaminoglycan Scaffolds Increases Osteogenic Gene Expression

To investigate the effects of cross-linking and nanoparticulate mineralization of C-GAG scaffolds on osteogenic differentiation of human MSCs, we measured the mRNA expression of osteocalcin (OCN) and bone sialoprotein (BSP) at 1, 7, and 14 days in culture (Figs. 1–2). In nonmineralized scaffolds, OCN mRNA expression did not change in a statistically significant manner in the absence or presence of cross-linking (C-GAG and XC-GAG, respectively). On days 7 and 14, cross-linking in C-GAG scaffolds actually resulted in a decrease in OCN expression. There were no statistically significant differences between noncross-linked and cross-linked mineralized scaffolds. Interestingly, nanoparticulate mineralized scaffolds (MC-GAG and XMC-GAG) had higher OCN expression than their respective counterparts at each timepoint in a statistically significant manner suggesting that mineralization of scaffolds promoted osteogenic differentiation of hMSCs (Fig. 1).

Bone sialoprotein mRNA expression also did not differ in a statistically significant manner in the absence or presence of cross-linking at any timepoint (Fig. 2). Both MC-GAG and XMC-GAG groups had higher BSP expression than their respective nonmineralized counterparts at each timepoint in a statistically significant fashion (Fig. 2). These data suggest that hMSCs seeded on mineralized scaffolds increase expression of OCN and BSP whereas cross-linking demonstrated a decrease in OCN expression with time.

Cross-linking Prevents Contraction of Scaffolds Seeded with Human Mesenchymal Stem Cells in Osteogenic Medium

To investigate scaffold contraction in the setting of cross-linking and mineralization, scaffold sizes were measured (in triplicate) after 5 weeks of culture with hMSCs in osteogenic medium (Table 2 and Fig. 3). Scaffold sizes in the C-GAG group decreased to 34.4 % of its original size of 8 mm in diameter. In the XC-GAG group, scaffold sizes decreased to 68.8% of its original size. The difference in contraction between the noncross-linked and cross-linked group was statistically significant. Likewise, the MC-GAG scaffolds decreased to 46.9% and XMC-GAG in contraction between nonmineralized and mineralized scaffolds were also compared. Mineralization resulted in a modest, but statistically significant decrease in contraction when C-GAG was compared with MC-GAG. The differences in contraction, however, were not statistically significant when scaffolds were cross-linked (XC-GAG versus XMC-GAG, $P = 0.35$). Thus, cross-linking significantly prevented contraction whereas mineralization had minimal effects on contraction of scaffolds seeded with hMSCs in osteogenic medium.

Nanoparticulate Mineralization of Collagen-Glycosaminoglycan Scaffolds Increases Mineralization of Human Mesenchymal Stem Cells Cultured in Osteogenic Medium

To elucidate the ability for cross-linking or nanoparticulate mineralization of C-GAG scaffolds to support in vitro mineralization of hMSCs cultured in osteogenic medium, hMSCs cultured on C-GAG and XC-GAG scaffolds for 8 weeks in triplicate in osteogenic medium were subjected to micro-CT scanning (Fig. 4). Similar to the physical

measurements taken of scaffolds in culture (Table 2), cross-linking resulted in decreased scaffold contraction. Cross-linking, however, also decreased the density of mineralization (Fig. 4B) in a statistically significant fashion. Mineralized collagen-glycosaminoglycan and XMC-GAG scaffolds were similarly subjected to 8 weeks of culture and micro-CT scanning in triplicate (Fig. 5). Again, cross-linking demonstrated decreased scaffold contraction. Decreased density of mineralized content was also seen when scaffolds were cross-linked (Fig. 5B) in a statistically significant fashion. These data demonstrated that cross-linking effectively prevents contraction at the cost of decreased mineralized volume. Lastly, we compared the differences in hMSC mineralization in the absence and presence of nanoparticulate mineralized scaffolds. Because of the significant contraction in noncross-linked scaffolds, we compared only XC-GAG versus XMC-GAG in triplicate. In comparison to empty scaffolds, mineralized content was increased in XMC-GAG ($10.3\% \pm 2.8\%$) versus XC-GAG ($5.5\% \pm 0.2\%$) scaffolds after 8 weeks of culture of hMSCs in osteogenic medium. Thus, nanoparticulate mineralized C-GAG scaffolds resulted in increased in vitro osteogenesis of hMSCs.

DISCUSSION

The conceptual approach to bone tissue engineering is to direct regeneration by applying osteogenic factors to a specific three-dimensional space. Current methods used to accomplish this concept usually include 2 elements: cellular material and scaffolding material.^{12,13} Strategic placement of the proper combination of cells and growth factors can support both recruitment of osteogenic cells from the host environment and osteogenesis on the scaffold. Contemporary bone tissue engineering research aims to optimize the delivery of the 2 components to generate a stable quantity of bone that fully integrates into the human body and sustains the test of time.

Many investigators have confirmed the importance of scaffold material and the specific properties of scaffolds in determining stem cell fate and osteogenesis.^{14,15} Techniques to stiffen the structure of C-GAG scaffolds by cross-linking have been described.⁸ In addition, nanoparticulate incorporation of calcium phosphate on C-GAG scaffolds has been developed in an effort to mimic the structure of native bone.⁷ Both of these techniques may be important steps to creating the optimal, clinically relevant scaffold material. In this work, we specifically investigated the contributions of cross-linking and nanoparticulate mineralization in osteogenesis of hMSCs and scaffold contraction. To that end, we examined gene expression of osteogenic genes and hMSC-directed mineralization in mineralized versus nonmineralized collagen scaffolds currently under development for orthopedic insertion repair.⁹

The rationale behind considering scaffold modifications is that our previous work demonstrated excellent promise for the utility of collagen-based scaffolds, albeit with the cost of scaffold contraction. This contraction is a significant deterrent to clinical translation for at least 2 reasons: difficulty in predicting the final dimensions of engineered bone; and inability to regulate the density and porosity of engineered bone. Both may cause potential problems in cellular infiltration and angiogenesis from the host environment and, ultimately, effective clinical bone healing.

Using custom-made C-GAG scaffolds with and without cross-linking and nanoparticulate mineralization, we found that the 2 scaffold modifications resulted in some differential effects. Although both modifications allowed for osteogenesis of hMSCs, cross-linking appeared to demonstrate an inhibitory effect on osteocalcin gene expression with time and mineralization. At 8 weeks of culture, mineralization was clearly decreased in the cross-linked scaffolds when compared with their noncross-linked counterparts ($P < 0.05$). This may be related to the method of cross-linking used in this study. For example, Keogh and colleagues have suggested differences in osteoblastic cell maturation depending on the type of cross-linking utilized and the final stiffness of the cross-linked scaffold.¹⁴ The major contribution of cross-linking, however, is that it indeed limited scaffold contraction in both nonmineralized and nanoparticulate mineralized C-GAG scaffolds.

Nanoparticulate mineralization, on the contrary, had a significant, reproducible response in promoting osteogenic gene expression and mineralization. The singular change in scaffold production was made to mimic the structure of native bone. Nanoparticulate mineralization did not prevent scaffold contraction, although the amount of contraction was slightly decreased in comparison to C-GAG scaffolds alone ($P < 0.05$). In combination, with cross-linking, nanoparticulate mineralized C-GAG scaffolds continued to exhibit increased osteogenic gene expression and mineralization. Calcium phosphate crystallites incorporated into the collagen scaffold may provide 2 discrete pro-osteogenic signals: increased scaffold stiffness¹⁶ and selective elution of Ca and P ions into the cell culture media.¹⁷ Although we have previously described the stiffness of these scaffolds variants,¹⁶ the modulus of the individual struts within the nonmineralized scaffolds have previously been shown to exceed 1 MPa,⁸ already in excess of substrates previously shown to increase MSC osteogenesis.¹⁸ Notably, we have previously demonstrated that upwards of 80% of the incorporated CaP content is released from the scaffold after 8 weeks of culture, with cross-linking not impacting mineral elution.¹⁷ Thus, the observed increase in new mineral synthesis in the MC-GAG versus C-GAG scaffolds reported here likely significantly underreports the osteogenic advantage conferred by the MC-GAG scaffolds. These results also are in agreement with recent observations that MC-GAG scaffolds can promote hMSC osteogenesis in the absence of osteogenic media supplementation (JCL, unpublished data). Therefore, cross-linked, nanoparticulate mineralized C-GAG scaffolds may be a biomaterial platform of great interest for further in vitro and in vivo studies, for consideration in clinical translation.

Acknowledgments

This work was supported by a Merit Review Grant (1I01BX001367-01A2) awarded by the U.S. Department of Veteran's Affairs (TAM), the Aramont Foundation, and the Jean Perkins Foundation (JCL). DWW was funded at UIUC from National Science Foundation (NSF) Grant 0965918 IGERT: Training the Next Generation of Researchers in Cellular and Molecular Mechanics and BioNanotechnology.

References

1. Ebraheim NA, Elgafy H, Xu R. Bone-graft harvesting from iliac and fibular donor sites: techniques and complications. *J Am Acad Orthop Surg.* 2001; 9:210–218. [PubMed: 11421578]
2. Arrington ED, Smith WJ, Chambers HG, et al. Complications of iliac crest bone graft harvesting. *Clin Orthop Relat Res.* 1996:300–309. [PubMed: 8769465]

3. Heinemann C, Heinemann S, Bernhardt A, et al. Novel textile chitosan scaffolds promote spreading, proliferation, and differentiation of osteoblasts. *Biomacromolecules*. 2008; 9:2913–2920. [PubMed: 18771318]
4. Ishaug SL, Crane GM, Miller MJ, et al. Bone formation by three-dimensional stromal osteoblast culture in biodegradable polymer scaffolds. *J Biomed Mater Res*. 1997; 36:17–28. [PubMed: 9212385]
5. Kruger EA, Im DD, Bischoff DS, et al. In vitro mineralization of human mesenchymal stem cells on three-dimensional type I collagen versus PLGA scaffolds: a comparative analysis. *Plast Reconstr Surg*. 2011; 127:2301–2311. [PubMed: 21617464]
6. Caliarì SR, Weisgerber DW, Ramirez MA, et al. The influence of collagen-glycosaminoglycan scaffold relative density and microstructural anisotropy on tenocyte bioactivity and transcriptomic stability. *J Mech Behav Biomed Mater*. 2012; 11:27–40. [PubMed: 22658152]
7. Harley BA, Lynn AK, Wissner-Gross Z, et al. Design of a multiphase osteochondral scaffold. II. Fabrication of a mineralized collagen-glycosaminoglycan scaffold. *J Biomed Mater Res A*. 2010; 92:1066–1077. [PubMed: 19301274]
8. Harley BA, Leung JH, Silva EC, et al. Mechanical characterization of collagen-glycosaminoglycan scaffolds. *Acta Biomater*. 2007; 3:463–474. [PubMed: 17349829]
9. Caliarì SR, Harley BA. Structural and biochemical modification of a collagen scaffold to selectively enhance MSC tenogenic, chondrogenic, and osteogenic differentiation. *Adv Healthc Mater*. 2014; 3:1086–1096. [PubMed: 24574180]
10. Olde Damink LH, Dijkstra PJ, van Luyn MJ, et al. Cross-linking of dermal sheep collagen using a water-soluble carbodiimide. *Biomaterials*. 1996; 17:765–773. [PubMed: 8730960]
11. Caliarì SR, Harley BA. The effect of anisotropic collagen-GAG scaffolds and growth factor supplementation on tendon cell recruitment, alignment, and metabolic activity. *Biomaterials*. 2011; 32:5330–5340. [PubMed: 21550653]
12. Szpalski C, Wetterau M, Barr J, et al. Bone tissue engineering: current strategies and techniques—part I: scaffolds. *Tissue Eng Part B Rev*. 2012; 18:246–257. [PubMed: 22029448]
13. Szpalski C, Sagebin F, Barbaro M, et al. The influence of environmental factors on bone tissue engineering. *J Biomed Mater Res B Appl Biomater*. 2012; 101:663–675. [PubMed: 23165885]
14. Keogh MB, O'Brien FJ, Daly JS. Substrate stiffness and contractile behaviour modulate the functional maturation of osteoblasts on a collagen-GAG scaffold. *Acta Biomater*. 2010; 6:4305–4313. [PubMed: 20570642]
15. Murphy CM, Matsiko A, Haugh MG, et al. Mesenchymal stem cell fate is regulated by the composition and mechanical properties of collagen-glycosaminoglycan scaffolds. *J Mech Behav Biomed Mater*. 2012; 11:53–62. [PubMed: 22658154]
16. Weisgerber DW, Kelkhoff DO, Caliarì SR, et al. The impact of discrete compartments of a multi-compartment collagen-GAG scaffold on overall construct biophysical properties. *J Mech Behav Biomed Mater*. 2013; 28:26–36. [PubMed: 23973610]
17. Weisgerber DW, Caliarì SR, Harley BA. Selective addition of mineral into collagen scaffolds to enhance hMSC osteogenesis and matrix remodeling. *Acta Biomaterialia*. 2014 Submitted.
18. Engler AJ, Sen S, Sweeney HL, et al. Matrix elasticity directs stem cell lineage specification. *Cell*. 2006; 126:677–689. [PubMed: 16923388]

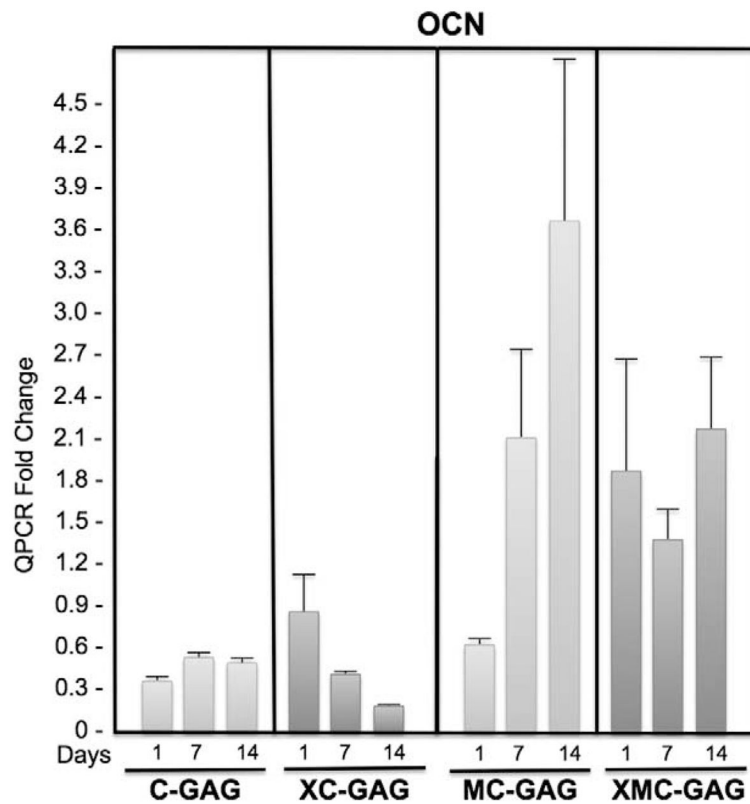


FIGURE 1.

Osteocalcin expression in collagen scaffolds. Human mesenchymal stem cells cultured on C-GAG, XC-GAG, MC-GAG, and XMC-GAG scaffolds in osteogenic medium were subjected with quantitative real-time RT-PCR (QPCR) for osteocalcin expression. Transcript fold changes from time zero are reported. C-GAG, collagen-glycosaminoglycan scaffold; MC-GAG, mineralized collagen-glycosaminoglycan scaffold; RT-PCR, reverse-transcriptase-polymerase chain reaction; XC-GAG, cross-linked collagen-glycosaminoglycan scaffold; XMC-GAG, cross-linked mineralized collagen-glycosaminoglycan scaffold.

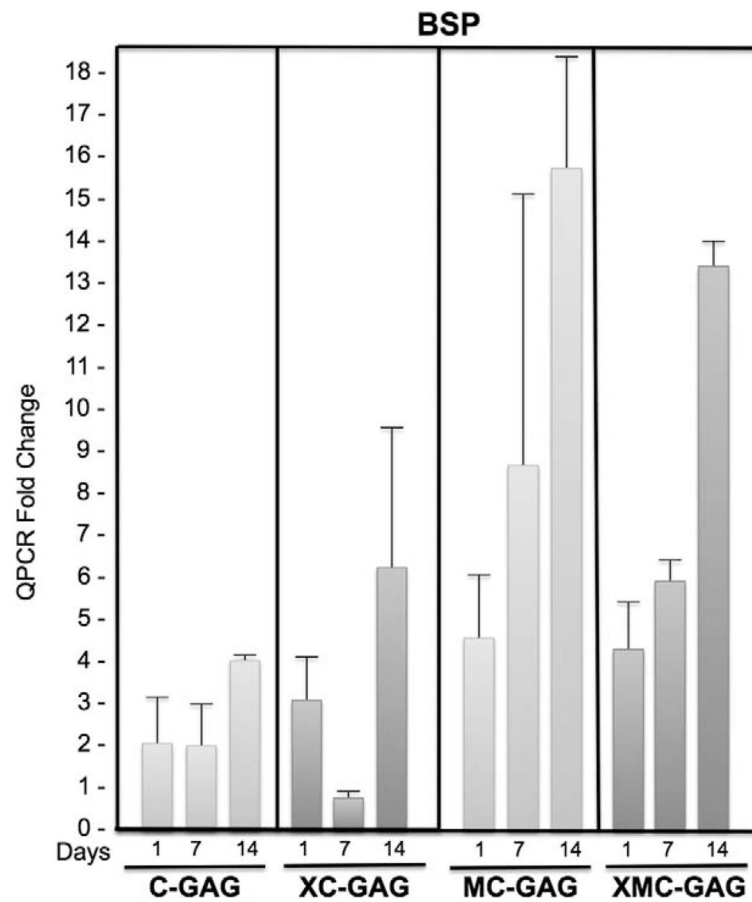


FIGURE 2.

Bone sialoprotein expression in collagen scaffolds. Human mesenchymal stem cells cultured on C-GAG, XC-GAG, MC-GAG, and XMC-GAG scaffolds in osteogenic medium were subjected with quantitative real-time RT-PCR (QPCR) for bone sialoprotein expression. Transcript fold changes from time zero are reported. C-GAG, collagen-glycosaminoglycan scaffold; MC-GAG, mineralized collagen-glycosaminoglycan scaffold; RT-PCR, reverse-transcriptase-polymerase chain reaction XC-GAG, cross-linked collagen-glycosaminoglycan scaffold; XMC-GAG, cross-linked mineralized collagen-glycosaminoglycan scaffold.

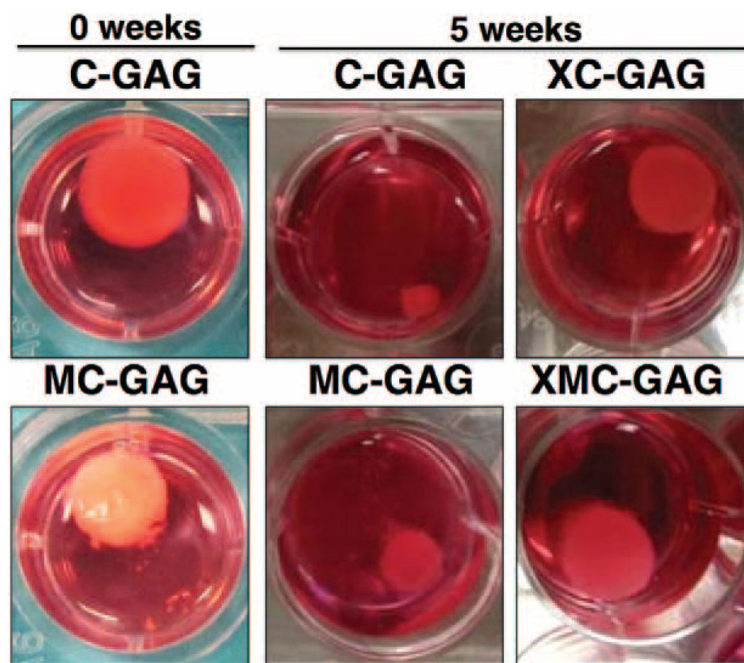


FIGURE 3.

Contraction of collagen scaffolds in culture. Photographs of hMSCs cultured on C-GAG, XC-GAG, MC-GAG, and XMC-GAG scaffolds in osteogenic medium for 5 weeks. Photographs of representative scaffolds are shown and scaffolds at time 0 without cross-linking are shown for comparison. C-GAG, collagen-glycosaminoglycan scaffold; MC-GAG, mineralized collagen-glycosaminoglycan scaffold; XC-GAG, cross-linked collagen-glycosaminoglycan scaffold; XMC-GAG, cross-linked mineralized collagen-glycosaminoglycan scaffold.

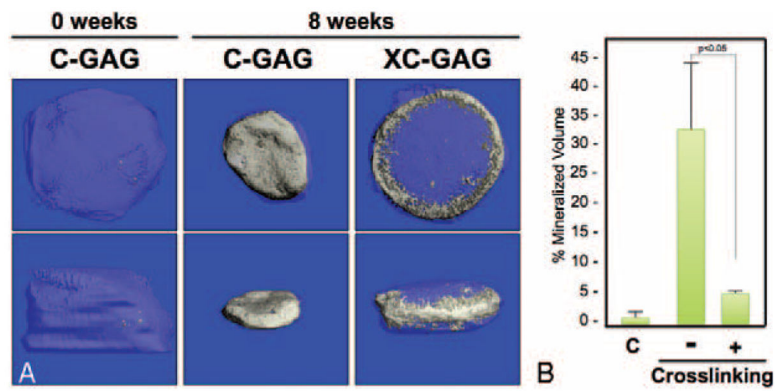


FIGURE 4.

Micro-CT comparison of mineralization of C-GAG and XC-GAG. Human mesenchymal stem cells cultured on C-GAG and XC-GAG scaffolds in osteogenic medium for 8 weeks were subjected to micro-CT scanning in triplicate. A, Top and side views of representative scaffolds are shown. B, The average percentage of mineralization of each scaffold was recorded. C, Control. C-GAG, collagen-glycosaminoglycan scaffold; MC-GAG, mineralized collagen-glycosaminoglycan scaffold; Micro-CT, microcomputed tomography; XC-GAG, cross-linked collagen-glycosaminoglycan scaffold; XMC-GAG, cross-linked mineralized collagen-glycosaminoglycan scaffold.

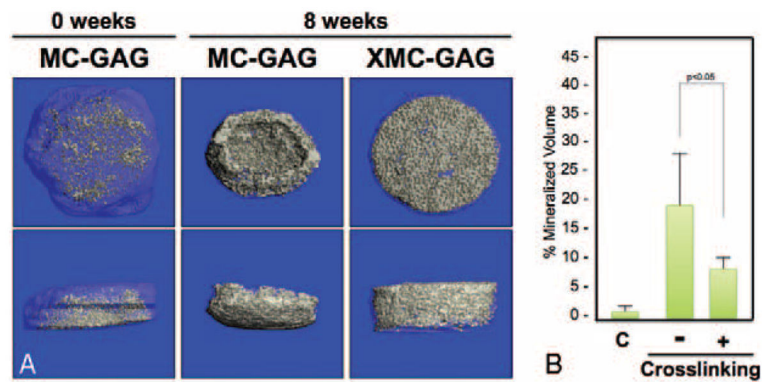


FIGURE 5. Micro-CT comparison of mineralization of MC-GAG and XMC-GAG. Human mesenchymal stem cells cultured on MC-GAG and XMC-GAG scaffolds in osteogenic medium for 8 weeks were subjected to micro-CT scanning in triplicate. A, Top and side views of representative scaffolds are shown. B, The average percentage of mineralization of each scaffold was recorded. C, Control. MC-GAG, mineralized collagen-glycosaminoglycan scaffold; Micro-CT, microcomputed tomography; XMC-GAG, cross-linked mineralized collagen-glycosaminoglycan scaffold.

TABLE 1**Human Primer Sequences**

Human Primer Sequences	Gene of Interest Oligonucleotide Sequence
18S rRNA sense	5'-CGGGTCATAAGCTTCGTT-3'
18S rRNA antisense	5'-CCGCAGGTTCACCTACGG-3'
OCN sense	5'-ATGATGGGGACCCACATCCATAG-3'
OCN antisense	5'-GTGTCGCTCTGCTGGCCTGG-3'
BSP sense	5'-TGG AAA TCG TTT TAA ATG AGG ATA-3'
BSP antisense	5'-AAG CAA TCA CCA AAA TGA AGA CT-3'

BSP, bone sialoprotein; OCN, osteocalcin.

TABLE 2

Scaffold Sizes Expressed as a Percentage of Original Scaffold Diameter in C-GAG, XC-GAG, MC-GAG and XMC-GAG Groups at 5 Weeks

	C-GAG	XC-GAG	<i>P</i> Value (Cross-linked Versus Noncross-linked)
Size (%)	34.4 ± 4.4	68.8 ± 8.8	0.02
	MC-GAG	XMC-GAG	
Size (%)	46.9 ± 4.4	71.9 ± 4.4	0.01
<i>P</i> value (mineralized versus nonmineralized)	0.04	0.35	

C-GAG, collagen-glycosaminoglycan scaffold; MC-GAG, mineralized collagen-glycosaminoglycan scaffold; XC-GAG, cross-linked collagen-glycosaminoglycan scaffold; *XMC-GAG, cross-linked mineralized collagen-glycosaminoglycan scaffold.